Alkali motion in alkali silicate glass

Akira Doi

Department of Inorganic Materials, Nagoya Institute of Technology, Nagoya 466, Japan
(Received 15 March 1978; accepted for publication 11 August 1978)

Alkali motion in alkali silicate glass was studied by the method of ionic thermocurrent which was developed as a highly sensitive technique for studying relaxation of polarized impurity-vacancy dipoles in ionic crystals. Two current peaks were observed in the temperature range −196–100°C, and were ascribed to orientational depolarization of pseudodipoles composed of localized alkali–nonbridging oxygen and to thermal relaxation of space charges near the cathode. Heterogeneous distribution of alkalis in alkali silicate glass was verified by large differences in ionic thermocurrent and in the evaluated density of localized alkalis from sample to sample taken from even the same glass film, as well as by the distribution in activation energies for dipolar orientation and space-charge relaxation. It was also concluded that the neutralization process of alkalis in glass was due to tunneling of electrons through the potential barrier in the space-charge–electrode double layer.

PACS numbers: 61.40.Df, 81.40.Rs, 66.30.Dn

INTRODUCTION

Alkali motion in alkali silicate glass has been studied so far mainly by measurements of electrical conduction and dielectric relaxation.[1-3] However, since both tools are insufficient to discriminate several overlapping processes which occur in relation to ionic motion, various explanations were made[3-8] to corrrelate them.

The purpose of the present work is to gain further insight into dynamic motion of alkalis in alkali silicate glass by the method of ionic thermocurrent (ITC) which was previously developed as a highly sensitive technique for studying relaxation of polarized impurity-vacancy dipoles in ionic crystals.[9-12] In this technique, the dipole system is polarized in a strong electric field in a temperature range in which dipole reorientation is readily possible, and then cooled (under field) to a temperature of frozen-in dipole reorientation. In a subsequent heating process (without applied field) the thermally activated depolarization of the dipole system occurs and is detected by measurement of the depolarization current.

In alkali silicate glasses, some of charge carriers are said to be localized and cannot contribute to electrical conduction.[8] When the above technique is applied to those glasses, it is very probable that pseudodipoles composed of localized alkali and nonbridging oxygen give rise to ITC on depolarization. Besides, due to ionic conduction, space charges are formed near the electrode (s). Some of them are neutralized, some remaining unneutralized would rediffuse into bulk on subsequent heating. We will show below that the observed ITC in alkali silicate glass can be explained in terms of rediffusion of alkalis piled up near the cathode and thermal relaxation of polarized pseudodipoles. Space charges affect various electrical measurements in crystals as well as in glasses. Although ITC due to relaxation of space charges was rarely reported,[13,14] It will soon be verified that the technique is very valuable for the study of space charges.

THEORETICAL

A theory of ionic conduction in glass[1,2] is extended to include the distribution in activation energies for conduction, as

$$j \approx \frac{e^2\lambda^2 E\nu}{2kT}\int_0^\infty n(H)\exp\left(-\frac{H}{kT}\right)dH \qquad (1)$$

when an unequality $eE\lambda \ll 2kT$ holds, where j is the current density, E is an applied field, λ is the average jumping distance in the direction of applied field, ν is the jumping frequency, H is the activation energy for conduction, and $n(H)$ is the carrier density having an energy barrier H. In Eq. (1), the current density follows Ohmic behavior. However, Ohm's law holds strictly true only when charge carriers which arrive at the cathode are all neutralized and simultaneously charge carriers are injected from the anode at an identical rate, that is, only when no space charges are formed near the electrode(s). In the present case, it is almost impossible to obtain Ohmic contact, rather the glass-electrode interface is imagined to be a blocking or partially blocking contact.[15-18]

Some of space charges thus piling up near the cathode are neutralized by electrons from the cathode. Neutralized charge carriers diffuse and coagulate to form colloids[17] in order to lower the interfacial free energy, or chemically react with ambient species such as adsorbed water.[19] Some remaining unneutralized charge carriers are, on the other hand, frozen-in by quenching the sample, but can rediffuse into bulk on subsequent heating. It is assumed here that space-charge carriers are crammed linearly along the extension of each chain of serial sites available for mobile alkalis, rather than homogeneous buildup in the space-charge region. If the motive force for rediffusion is Coulombic repulsion among space-charge carriers, the repulsive force should be proportional to $1/r^2$, where r is an interalkali distance in alkali chains in the space-charge region. Since linear cram-

 0021-8979/79/031291-07$01.10

ming of alkalis infers inverse dependence of r on the space-charge density n, the repulsive force should be proportional to n^2. Then a differential current dj' due to relaxation of space-charge carriers of the density $n(H)$ having activation energies in the range $H \sim H + dH$ is given by

$$dj' = -\frac{dn(H)}{dt}dH = cn(H)^2\nu \exp\left(-\frac{H}{kT}\right)dH, \quad (2)$$

where c is a constant. The overall depolarization current due to relaxation of space charges during warm-up at a rate of $T = T_0 + \beta t$ is, therefore,

$$j' = \int_{H=0}^{H=\infty} dj'$$

$$= \int_0^\infty c\nu \exp\left(-\frac{H}{kT}\right)\left[\frac{1}{n_0(H)} + \frac{c\nu}{\beta}\int_{T_0}^{T} \exp\left(-\frac{H}{kT}\right)dT\right]^{-2} dH, \quad (3)$$

where $n_0(H)$ is the frozen-in space-charge density at T_0 having an activation energy H. Equation (3) implies that the peak temperature of the relevant ITC should vary with $n_0(H)$, that is, with polarizing conditions used. When the variation of H is small in an early stage of ITC, the following relation holds:

$$\ln j' = \text{const} - H/kT. \quad (4)$$

The slope of a logarithmic plot of j' against the inverse temperature would yield the value of dominant activation energy (the initial rise method[9]). Some information about distribution in activation energies can be obtained by applying the method after partial cleaning of charge carriers having lower H, i.e., instead of recording the whole ITC at one time, one should first discharge the lower-temperature tail, quench the sample, discharge next to progressively higher temperatures, and each fragment of the whole ITC is analyzed by Eq. (4).

We consider next the orientational polarization of alkali–nonbridging oxygen pseudodipoles under an applied field E_p at a polarization temperature T_p. If $P(H)$ is a polarization by pseudodipoles of the density $n(H)$, a differential current dj'' due to pseudodipoles having activation energies in the range $H \sim H + dH$ is[2]

$$dj'' = \frac{dP(H)}{dt}dH = \frac{P_\infty(H) - P(H)}{\tau}dH, \quad (5)$$

where

$$P_\infty(H) = \frac{n(H)p^2\alpha E_p}{kT_p} \quad (6)$$

is the saturated polarization when $pE_p \ll kT_p$, and

$$\tau = \tau_0 \exp(H/kT) \quad (7)$$

is the relevant relaxation time, τ_0 is a constant, p is the dipole moment, and α is the geometrical factor. The factor α depends on the possible dipolar orientation and is one-third for freely rotating dipoles and unity for dipoles having only two possible orientations, i.e., parallel or antiparallel direction to E_p. Since our pseudodipoles can rotate to any direction in principle, $\alpha = \frac{1}{3}$. An overall current due to polarization of pseudodipoles having distribution in activation energies is

$$j'' = \int_{H=0}^{H=\infty} dj''$$

$$= \frac{p^2E_p}{3kT_p}\int_0^\infty \frac{n(H)}{\tau}\exp\left(-\frac{t}{\tau}\right)dH. \quad (8)$$

After polarizing the system at T_p for a properly chosen polarization time t_p, the sample is cooled to T_0. After the removal of E_p at T_0, the temperature is raised with constant rate $\beta = dT/dt$, and the thermally stimulated depolarization current due to relaxation of frozen-in dipoles is[10]

$$j''' = \frac{p^2E_p}{3kT_p}\int_0^\infty \frac{n(H)}{\tau(T)}\left[1 - \exp\left(-\frac{t_p}{\tau(T_p)}\right)\right] \times \exp\left(-\int_{T_0}^{T}\frac{dT}{\beta\tau(T)}\right)dH. \quad (9)$$

Equations (8) and (9) indicate that both j'' and j''' follow Ohmic behavior when the related process is orientational polarization or depolarization of pseudodipoles. As in the case of relaxation of space charges discussed above, Eq. (9) shows that partial cleaning followed by the initial rise analysis would give information on the distribution in H.

EXPERIMENTAL

Glass samples were of the composition Li_2O-$2SiO_2$, Na_2O-$2SiO_2$, or $(LiO_{1/2}$-$NaO_{1/2})$-$2SiO_2$. We abbreviated them as L2S, N2S, and LN2S. Sample numbers were labeled as L2S(a), L2S(b), etc. Glass films 4–10 μm thick were pre-

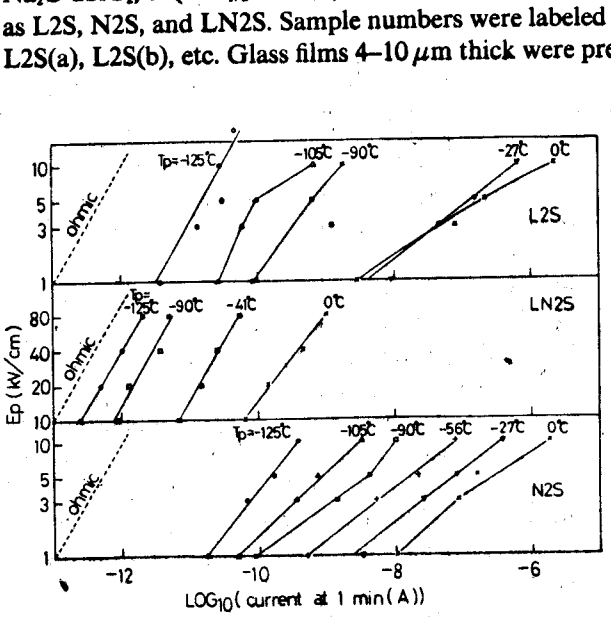

FIG. 1. The charging current at 1 min after applying E_p under various polarizing conditions of T_p and E_p on L2S (g), LN2S (a), and N2S (a). Ohmic slope is indicated by the dotted curve.

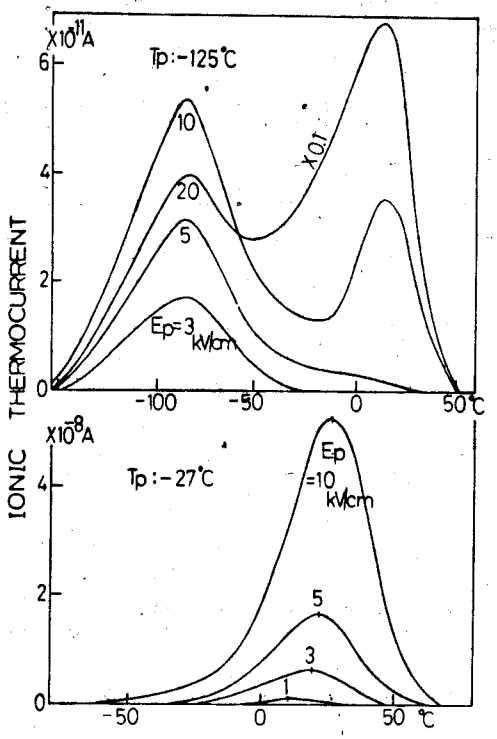

FIG. 2. Typical ITC curves of N2S(a) polarized at -125 and at -27 °C under various E_p. As is apparent, P1 is gradually overwhelmed by the growing P2 with T_p and E_p.

pared by blowing melt of high-purity materials by oxygen. The electrodes were evaporated gold or aluminum on both sides of the samples of dimension 2 cm × 2 cm × (4–10) μm. The cryostat used to measure ITC was evacuated by an oil-diffusion pump having liquid-nitrogen traps. A copper-constantan thermocouple glued in the sample holder made of copper measured the temperature. Electrical measurements were made with a Takeda-Riken TR 84M vibrating reed electrometer or TR 8651 electrometer. The procedure to measure ITC was as follows: (i) The sample was biased by E_p at T_p for t_p ($= 2$ or 5 min), (ii) rapidly cooled to T_0 (-196 °C) within 3 min under E_p, where the cooling time of 3 min was sufficient to give negligible disturbance to t_p since decay of the charging current was large within initial cooling, and (iii) after an appropriate time at T_0, E_p was switched off, and the sample was heated at a rate of $\sim$0.058 °C/sec up to 100 °C. Since the induced current in the measured temperature range was far less than 10^{-13} A when samples were zero-biased or when studies were made on high-resistivity alumina, it was concluded that the observed ITC was due primarily to the motion of charge carriers in glass samples.

RESULTS AND DISCUSSION

Figure 1 shows the charging current at 1 min after applying E_p on three glasses at different T_p. As is apparent in Fig. 1, LN2S has a higher electrical resistivity than L2S or N2S due to the mixed alkali effect in glass,[20] a phenomenon that the mobility of alkalis decreases when they are progressively substituted by different alkalis or pseudoalkalis or even their isotopes. In the experimental condition used, an unequality $eE_p\lambda \ll 2kT_p$ or $pE_p \ll kT_p$ holds. Therefore, if the charging current is due strictly to orientational polarization

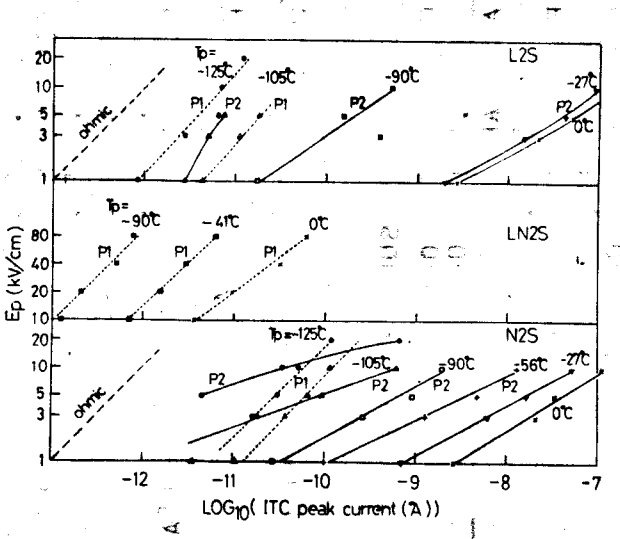

FIG. 3. E_p and T_p dependences of two (P1, P2) ITC peak currents for L2S(g), LN2S(a), and N2S(a). For all samples studied so far, P1 follows Ohmic behavior, while P2 is supralinear.

or to ionic conduction with Ohmic contact, we will observe Ohmic behavior [Eqs. (1) and (8)]. It is surely observed when T_p is low or when the sample resistivity is high, as in LN2S. When T_p is increased, however, deviation to supralinearity becomes noticeable.

Figure 2 shows typical ITC curves of N2S. In the measured temperature range two ITC peaks are observed, one is P1 which is dominant at low T_p, while the other is P2 which overwhelms P1 when T_p increases. A similar ITC curve is observed in L2S, as is expected from similar activation energies for conduction in L2S and N2S.[7] In LN2S, on the other hand, only one peak is detected under polarizing conditions (T_p,E_p,t_p) used, and is verified to be P1 through discussions given later. Figure 3 shows E_p and T_p dependences of the ITC peak current (I_m) for three glasses. Figures 4 and 5 show E_p dependences of the peak temperature (T_m) and I_m of two ITC peaks on L2S. If the observed ITC is due to orientational depolarization of pseudodipoles, T_m must be independent of E_p, and I_m must be proportional to E_p [Eq. (9)]. Figure 4 suggests that P1 corresponds to the prescribed process.

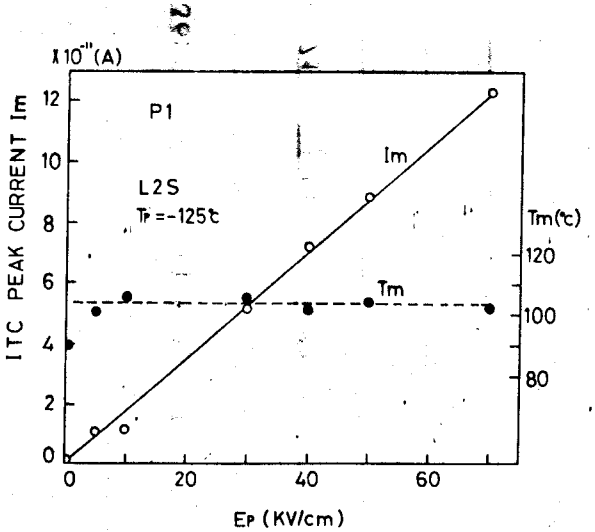

FIG. 4. E_p dependences of the peak temperature T_m and peak current I_m of P1 in L2S(h) at $T_p = -125$ °C where P1 is dominant.

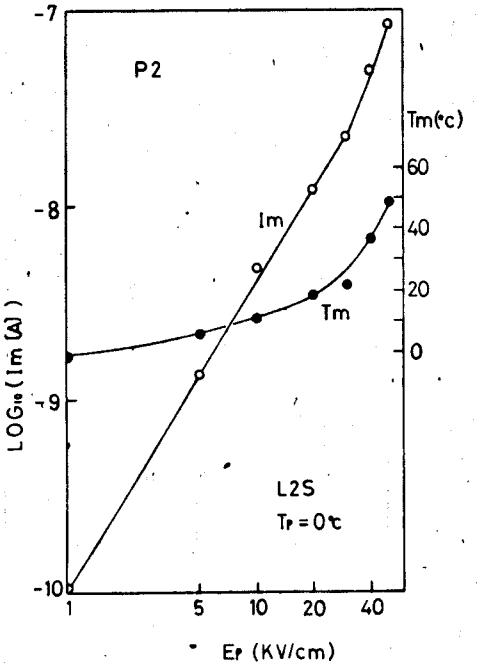

FIG. 5. E_p dependences of T_m and I_m of P2 in L2S(a) at $T_p = 0\,°C$ where P2 is dominant.

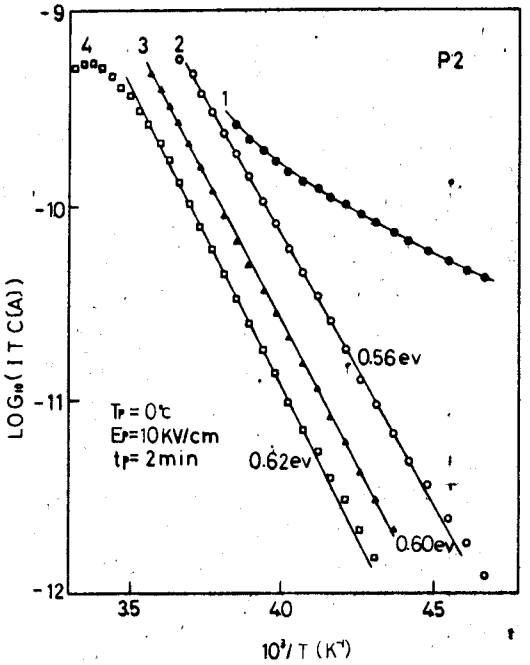

FIG. 7. Four cycles of intial rise analysis about P2 of L2S(j) after partial cleaning of charge carriers having lower activation energies. A dominant activation energy in each cycle comes close to 0.65 eV with cycles which is the activation energy for lithium conduction in L2S.

When the cycle of partial-cleaning–initial-rise analysis is repeated on P1 (Fig. 6), it is revealed that the process which corresponds to P1 has distribution in activation energies, namely, of the whole carriers giving rise to P1, 53% have $H < 0.26$ eV, 12% have $H \sim 0.26$ eV, and the remaining have $H \gtrsim 0.28$ eV. A similar treatment on P1 in LN2S reveals smaller activation energies than in L2S or N2S, i.e., 44% of the carriers have $H < 0.09$ eV, 8% have $H \sim 0.09$ eV, 11% have $H \sim 0.13$ eV, 10% have $H \sim 0.15$ eV, and 27% have $H > 0.15$ eV. Moreover, the carrier density in LN2S which

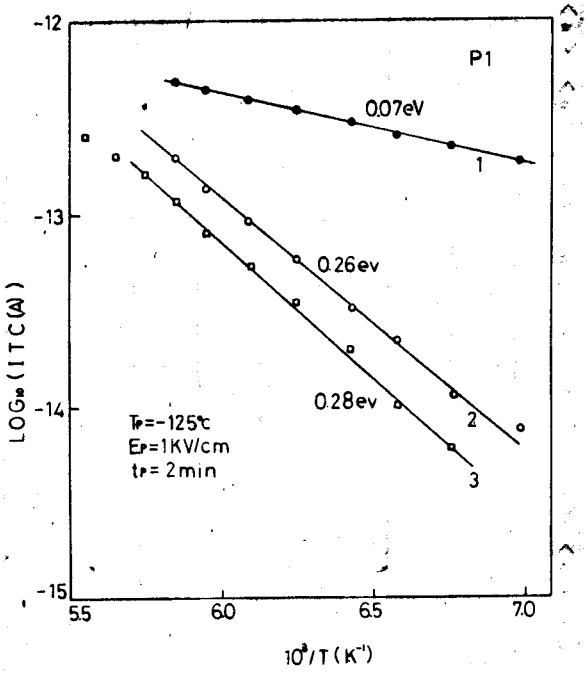

FIG. 6. Three cycles of initial rise analysis about P1 of L2S(h) after partial cleaning of charge carriers having lower activation energies. A dominant activation energy in each cycle is indicated in the figure.

contributes to P1 is about two orders of magnitude less than the carriers in L2S or N2S. Homogenized distribution of alkalis due to alkali mixing[20] may be responsible for the observed low density of the carriers in LN2S which contribute to P1. Meanwhile, the activation energy for P2 comes close to 0.65 eV which corresponds to lithium conduction in L2S as derived by measurements of electrical resistivity, dielectric loss,[7] or NMR.[21] Of all the carriers giving rise to P2 in L2S(j), 15% have $H < 0.56$ eV, 25% have $H \sim 0.56$, 16% have $H \sim 0.60$ eV, and the remaining 44% have $H \gtrsim 0.62$ eV (Fig. 7). As is evident from Figs. 4 and 5, P1 always follows Ohmic behavior, while P2 is supralinear. Also, the charging current at 1 min after applying E_p is Ohmic at low T_p, but deviates to supralinearity with increasing T_p (Fig. 1). These results lead us to reasonable assignment that P1 corresponds to orientational depolarization of pseudodipoles and P2 to thermal relaxation of space charges accumulated at the cathode.

Recently, it was inferred[8] that in glass some of charge carriers are localized and cannot contribute to electrical conductivity σ based on the difference between calculated and experimentally derived values of the ratio f_m/σ between σ and the dielectric loss peak f_m. Due to a large ambiguity in the reported values of f_m and σ,[7] however, even the rough estimate of the density of localized carriers (N_{loc}) is hardly possible at present. The ITC technique can, on the other hand, yield quantitative estimation of N_{loc}. The area S covered by P1 satisfies Eq. (10),

$$S = \frac{Np^2E_p}{3kT_p} \qquad (10)$$

when the polarization is saturated. Suppose N is the overall carrier density (e.g., 1.87×10^{22} cm^{-3} in L2S) and $p = er$ (e the elementary charge), then the distance r between lithium–

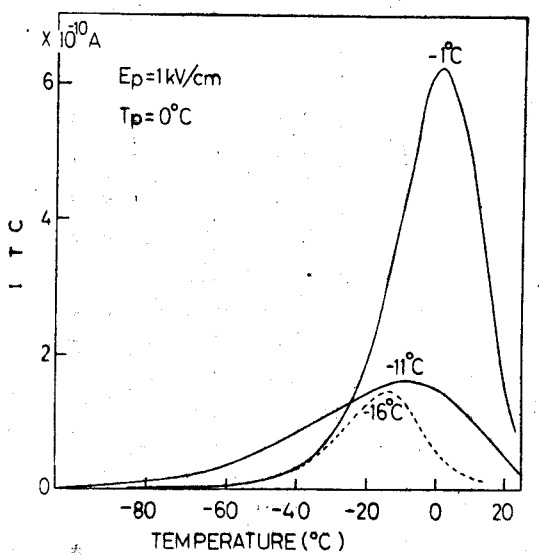

FIG. 8. ITC curves of L2S(k), L2S(l), and L2S(m) taken from the same blown film. Peak temperatures are shown atop each curve. A large scatter in ITC curves cannot be ascribed to any uncertainties in the measuring technique.

nonbridging oxygen in L2S (h) (Fig. 4) is calculated to be $r = 0.77 \pm 0.02$ Å. Meanwhile, the average distance of lithium–oxygen is 1.94 Å in monoclinic $Li_2Si_2O_5$.[22] Therefore, based on the assumption that only localized carriers contribute to P1 and that r is 1.94 Å or somewhat larger than this, N_{loc} is calculated to be $\lesssim 0.16N$. That is, 16% or less of the charge carriers are localized in L2S(h). Yet in L2S(g), for example, only 6% of the charge carriers are localized. Such a large scatter in N_{loc} favors the postulate that spatial distribution of mobile and immobile (localized) carriers varies from sample to sample. Alkali distribution in glass is imagined to be heterogeneous in the sense that any alkali ion finds its nearest-neighbor alkali at a distance which differs from site to site, so some alkalis are hard by steric hindrance to move long distances in the direction of applied field and therefore are localized. A supporting evidence is large differences in ITC curves from sample to sample taken from even the same blown film, as are exemplified for L2S in Fig. 8. In Fig. 9, normalized decay curves of the charging current are shown for L2S biased by $E_p < 40$ kV/cm at $T_p = -125$ °C where P1 is dominant. As is suggested from Eq. (8), no exponential decay of the charging current is observed, contrary to the expectation for the process with single activation energy.

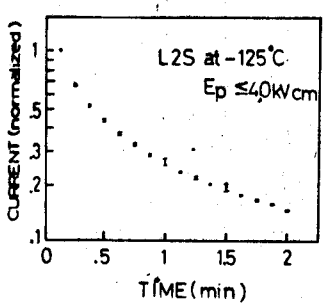

FIG. 9. Normalized decay curves of the charging current in L2S(h) when it is polarized by $E_p < 40$ kV/cm at -125 °C where P1 is dominant.

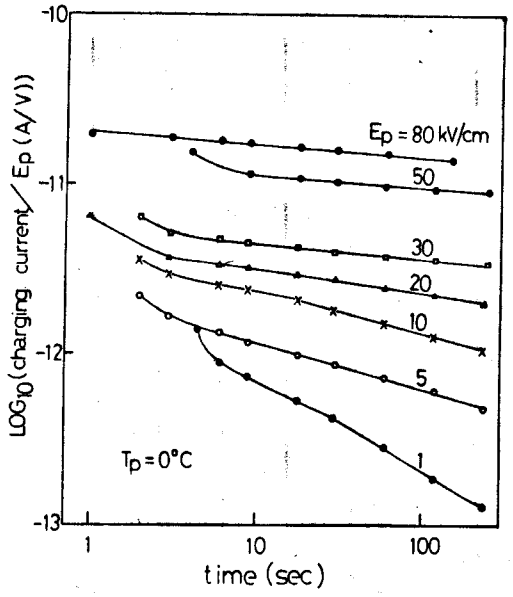

FIG. 10. Decay curves of the charging current in L2S(a) at various E_p at $T_p = 0$ °C where P2 is dominant.

Also noted is an independence of normalized decay curves on E_p, in fair agreement with Eq. (8).

Figure 10 shows decay curves of the charging current in L2S which is biased by various E_p at $T_p = 0$ °C, where P2 is dominant. An observed time decay may be due to retardation on moving alkalis by space charges piled up near the cathode.[15] However, the charging current becomes flattened under large E_p, due perhaps to an increased neutralization of

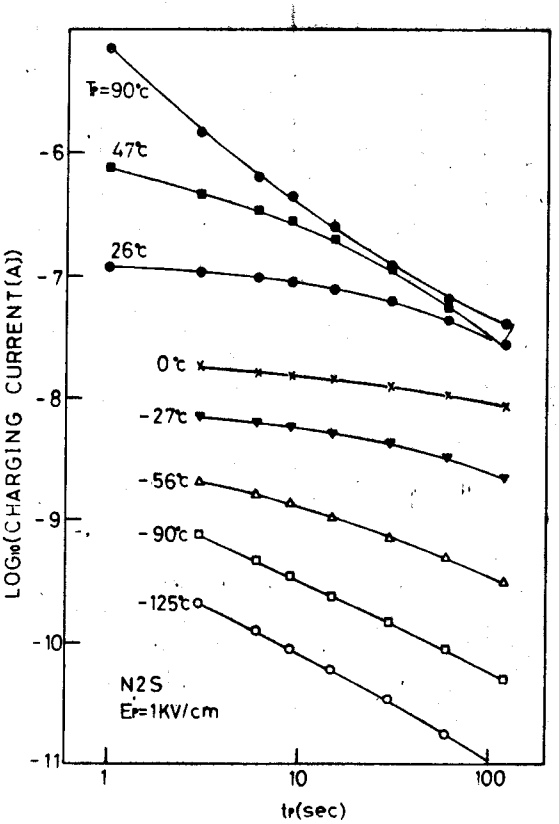

FIG. 11. Decay curves of the charging current in N2S(a) at various T_p and $E_p = 1$ kV/cm. An almost identical behavior was observed in L2S.

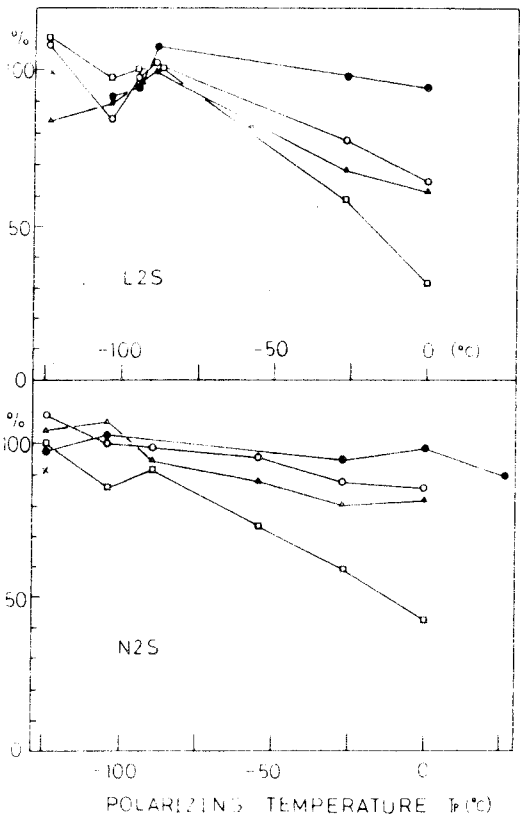

IG. 12. T_p and E_p dependences of the ratio Q_I/Q_C for L2S(g) and N2S(a), here E_p = 1 kV/cm (●), 3 kV/cm (○), 5 kV/cm (△), 10 kV/cm (□), and kV/cm (×).

ace charges with E_p. When the polarizing condition $_p,E_p,t_p$) becomes more severe, the potential drop across the pletion layer near the anode would come to play the leading role in the time decay of the charging current.[15] An expected decay is shown in Fig. 11 where, as T_p increases, the arging current becomes flattened first, but on further increase in T_p the time decay becomes again noticeable

Figure 12 shows T_p and E_p dependences of the ratio $_I/Q_C$ of the areas covered by the charging current (Q_C) and ITC (Q_I) of two glasses. In those glasses, P1 is dominant

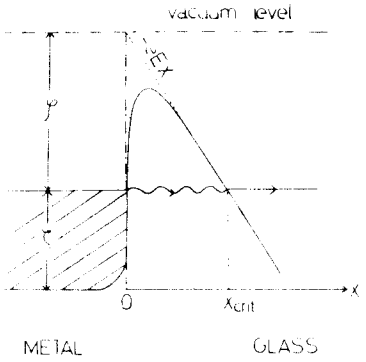

G. 13. Energy scheme at the glass-cathode interface. In the absence of ace charges, electrons at the Fermi level E_f face the potential barrier φ. As ce charges pile up on the glass surface, an electric field E formed in the ctrode–space-charge double layers lowers the barrier. When E grows h, the barrier width X_{crit} becomes thin enough for tunneling of electrons ccur. Electrons below or above E_f are ineffective due to increasing barr width or to negligible electron density.

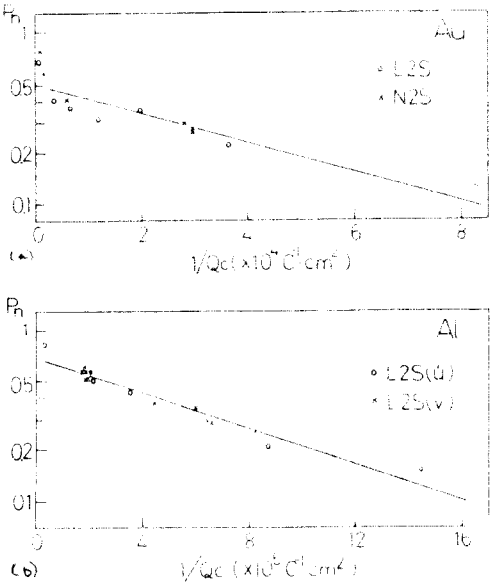

FIG. 14. Macroscopic neutralization probability P_n as a function of reciprocal Q_C for various samples of L2S and N2S with evaporated gold as electrodes (a) and for L2S(u) and L2S(v) with evaporated aluminum as electrodes (b).

at low T_p, so the ratio Q_I/Q_C lies at almost unity, but P1 is gradually overwhelmed by the growing P2 at higher T_p; thereby a parallel increase in the rate of the neutralization process lowers the ratio.

To understand this process, an examination of the neutralization mechanism is necessary. First, consider the possibility that neutralization proceeds via the potential barrier at the glass-cathode interface by lowering the barrier by an electric field formed in the electrode–space-charge double layer (Fig. 13). The electric field available in the double layer is

$$E = q/\epsilon_0\epsilon_r \tag{11}$$

where q is the space-charge density, ϵ_0 is the permittivity of free space, and ϵ_r is the dielectric constant in the layer. In the presence of applied field E, the contact-limited Schottky emission follows the formula[23]

$$j = AT^2 \exp(-\varphi/kT)\exp(\beta_s E^{1/2}), \tag{12}$$

where j is the emission current, φ is the work function of the electrode material, A is a constant, and $\beta_s = (e^3/\pi\epsilon_0\epsilon_r)^{1/2} \times (2kT)^{-1}$. Also possible is the neutralization process via tunneling of electrons from the cathode to glass through the potential barrier in the double layer, where the tunneling probability P_t is given by[24]

$$P_t \approx \frac{16\zeta\varphi}{(\zeta+\varphi)^2}\exp(-2\beta_t X_{crit}), \tag{13}$$

in which $\beta_t = (2m\varphi/\hbar^2)^{1/2}$, ζ is the Fermi energy of the cathode, and X_{crit} is the tunneling distance. Since the image force on the tunneling electron is negligible when E is large, the equation

$$(\zeta+\varphi) - eEX_{crit} \approx \zeta \tag{14}$$

holds, so that

$$X_{crit} \approx \varphi/eE. \quad (15)$$

Equations (13) and (15) give Fowler-Nordheim-type plots of $\ln P_t$ against $1/E$. P_t is equal to the tunneling fraction of incoming electrons onto the metal surface as attracted by space charges accumulating per unit time onto the glass surface. Therefore, strictly speaking, P_t should be equal to the neutralized fraction of space charges accumulating onto the glass surface per unit time. Fortunately, since time decay of the charging current varies only slightly under the polarizing conditions used (Figs. 10 and 11), the macroscopic neutralization probability P_n defined by the ratio $(Q_C - Q_I)/Q_C$ can be assigned approximately to P_t. Similarly, the space-charge density q in Eq. (11) can be taken to be proportional to Q_C. When these approximations are made, a linear dependence of $\ln P_n$ on the inverse Q_C is observed (Fig. 14). However, the Schottky plots of $\ln j$ versus $Q_C^{1/2}$ cannot give any linear portion when j is assigned to neutralized charges $Q_n (= Q_C - Q_I)$ or to P_n. It is, therefore, very plausible to say that the neutralization mechanism of charge carriers in the glass is due to tunneling of electrons through the potential barrier in the space-charge–electrode double layer. What we can say further at present is that (i) the neutralization probability is indifferent to whether the charge carriers are lithium or sodium ions and (ii) the probability depends strongly on the electrode material. When the ratio of work functions of aluminum (φ_{Al}) and gold (φ_{Au}) is calculated from Fig. 14 based on Eqs. (13) and (15), $\varphi_{Al}/\varphi_{Au} \approx 0.15$. This is far below the reported value of 0.80,[25,26] although the scatter is very large. This difference may be due to contamination in the present work as compared to an almost clean surface used in the reported experiments.

SUMMARY

The ITC technique has allowed us to resolve two different relaxation modes of alkalis in alkali silicate glass: the mode which is dominant at low T_p is orientational depolarization of pseudodipoles composed of localized alkali–nonbridging oxygen, and the other mode which is dominant at high T_p is thermal relaxation of space charges piled up near the cathode. Localized alkalis arise by heterogeneous distribution of alkalis in alkali silicate glass as is verified by large differences in ITC and in the evaluated density of localized alkalis from sample to sample taken from even the same glass film, as well as by the distribution in activation energies for two relaxation modes. We have shown also that the neutralization process of alkalis is due perhaps to tunneling of electrons from the cathode through the potential barrier in the space-charge–electrode double layer.

ACKNOWLEDGMENT

The helpful assistance of Masaki Takatsugi is gratefully acknowledged.

[1]J.M. Stevels, *Handbüch der Physik* (Springer, Berlin, 1957), Vol. 20, p. 350.
[2]A.E. Owen, Prog. Ceram. Sci. **3**, 77 (1963).
[3]M. Tomozawa, *Treatise on Materials Science and Technology* (Academic, New York, 1977), Vol. 12, p. 283.
[4]R.J. Charles, J. Appl. Phys. **32**, 1115 (1961).
[5]J.O. Isard, Proc. IEE Suppl. **22**, 109 (1962); **22**, 440 (1962).
[6]T. Nakajima, Conf. Electr. Insul. Dielect. Phenom., Williamsburg, 1971 (unpublished).
[7]H. Namikawa, J. Non-Cryst. Solids **18**, 173 (1975).
[8]A. Doi, J. Non-Cryst. Solids **29**, 131 (1978).
[9]C. Bucci and R. Fieschi, Phys. Rev. Lett. **12**, 16 (1964).
[10]C. Bucci and R. Fieschi, Phys. Rev. **148**, 816 (1966).
[11]C. Laj and P. Bergé, J. Phys. (Paris) **28**, 821 (1967).
[12]J.P. Stott and J.H. Crawford, Jr., Phys. Rev. B **4**, 639 (1971).
[13]C. Bucci and S.C. Riva, J. Phys. Chem. Solids **26**, 363 (1965).
[14]I. Thurzo and J. Doupovec, J. Non-Cryst. Solids **22**, 205 (1976).
[15]P.M. Sutton, J. Am. Ceram. Soc. **47**, 188 (1964).
[16]K.W. Hang and G.F. Stockdale, J. Am. Ceram. Soc. **55**, 338 (1972).
[17]S.P. Mitoff and R.J. Charles, J. Appl. Phys. **43**, 927 (1972).
[18]J.R. Macdonald, J. Appl. Phys. **44**, 3455 (1973).
[19]R.H. Doremus, J. Non-Cryst. Solids **19**, 137 (1976).
[20]J.O. Isard, J. Non-Cryst. Solids **1**, 235 (1969).
[21]J.R. Hendrickson and P.J. Bray, J. Chem. Phys. **61**, 2754 (1974).
[22]F. Liebau, Acta Crystallogr. **14**, 389 (1961).
[23]J. Antula, Phys. Status Solidi **28**, 395 (1968).
[24]L.I. Schiff, *Quantum Mechanics* (McGraw-Hill, New York, 1955), p. 92.
[25]V.S. Fomenka, *Handbook of Thermionic Properties* (Plenum, New York, 1966).
[26]H.B. Michaelson, J. Appl. Phys. **48**, 4729 (1977).